606-nm InGaN Amber Micro-Light-Emitting Diodes With an On-Wafer External Quantum Efficiency of 0.56%

Zhe Zhuang, Daisuke Iida, Martin Velazquez-Rizo, and Kazuhiro Ohkawa, *Member, IEEE*

***Abstract*— We demonstrated amber InGaN 47 × 47 μm^2 micro-light-emitting diodes (μLEDs) with the peak wavelength of 606 nm and full-width at maximum (FWHM) of 50 nm at 20 A/cm^2. The amber μLEDs exhibited a 33-nm blue-shift of the peak wavelength and obtain broader FWHMs to approximately 56 nm at 5 to 100 A/cm^2. The peak on-wafer external quantum efficiency was 0.56% at 20 A/cm^2. The characteristic temperature was 50–80 K at 20 to 60 A/cm^2 but increased to 120–140 K at 80 to 100 A/cm^2. The strong increase in the characteristic temperature from 60 to 80 A/cm^2 could mainly be attributed to the saturation of the Shockley-Read-Hall non-radiative recombination at high current densities.**

***Index Terms*— InGaN, amber micro-light-emitting diode, on-wafer external quantum efficiency, characteristic temperature.**

I. Introduction

DUE to their high brightness levels, long lifetime, large modulation bandwidth, and small form factors, InGaN-based micro-light-emitting diodes (μLEDs) have achieved expanding interests in many newly-emerging applications such as micro-displays in wearable and smart electronics, visible light communication, and biomedical sensors [1,2]. Although InGaN blue and green LEDs have been commercialized owing to their mature technology and reliability, many studies have reported that the external quantum efficiency (EQE) of InGaN μLEDs decreases with chip size [3]–[5]. This size dependence of the EQE was caused by the non-radiative recombination at the edge of the device active region [6]–[8], which could be eliminated or avoided by using a combination of chemical treatment and atomic-layer deposition sidewall passivation [9] or the bottom-up growth method to form μLED mesas [10].

Manuscript received April 27, 2021; revised May 12, 2021; accepted May 13, 2021. Date of publication May 17, 2021; date of current version June 29, 2021. This work was supported in part by the King Abdullah University of Science and Technology (KAUST) under Grant BAS/1/1676-01-01 and in part by the Nanofabrication Core Laboratory, KAUST. The review of this letter was arranged by Editor T.-Y. Seong. *(Corresponding author: Kazuhiro Ohkawa.)*

The authors are with the Computer, Electrical and Mathematical Sciences and Engineering (CEMSE) Division, King Abdullah University of Science and Technology (KAUST), Thuwal 23955, Saudi Arabia (e-mail: zhe.zhuang@kaust.edu.sa; daisuke.iida@kaust.edu.sa; martin.velazquezrizo@kaust.edu.sa; kazuhiro.ohkawa@kaust.edu.sa).

Color versions of one or more figures in this letter are available at https://doi.org/10.1109/LED.2021.3080985.

Digital Object Identifier 10.1109/LED.2021.3080985

Another important issue to consider is red, green, and blue μLEDs for full-color micro-displays. Generally, InGaN LEDs suffer from a significant reduction in EQE as the In content increases in InGaN quantum wells (QWs) [11]. EQE reduction can mainly be attributed to the degradation of the crystal quality for InGaN QWs because of the large lattice mismatch between high In-content InGaN and GaN templates [8]. To reduce lattice mismatch, a partially relaxed InGaN pseudo-substrate fabricated by Soitec was proposed for high In-content InGaN red LEDs [12]. Another lattice-matched InGaN template grown on $ScAlMgO_4$ (0001) substrates also proved to be capable of remarkably improving the internal quantum efficiency of InGaN QWs, showing the potential of these lattice-matched templates for long-wavelength InGaN emitters [13].

Recently, 6 × 6 μm^2 size 632-nm InGaN μLEDs on porous GaN were demonstrated to have an on-wafer EQE of 0.2%, which was the first reported value for red μLEDs with the dimension <10 μm [14]. Besides, orange/red InGaN LEDs could realize high efficiency on silicon substrates [15] because the tensile strain of the GaN on silicon during growth was favorable for In incorporation [11]. Our group chose to adjust the thickness of the GaN on sapphire substrates to realize highly efficient InGaN red LEDs [16]. Besides, the proposed micro-flow growth method [17] and AlN/AlGaN strain-compensated barriers [18] were also useful for improving the crystal quality of high-In-content InGaN QWs.

For most micro-displays, μLEDs need to be driven at low current densities. However, some applications such as head-mounted displays and image sources in projection systems, which need very high brightness levels, require μLEDs to be operated at high current densities. Besides, the optogenetic stimulation of chrimson by μLEDs also requires a minimal optical power density, which could not be realized at low current densities [19]. Because strong quantum-confined Stark effect (QCSE) in InGaN QWs makes a large blue-shift of the peak wavelength, InGaN long-wavelength-emitting μLEDs operated at high current densities need higher In contents compared to μLEDs operated at low current densities, which will be much more challenging.

In this work, we demonstrated 606-nm InGaN amber μLEDs with dimensions of 47 × 47 μm^2 at 20 A/cm^2. We examined the current–voltage (I–V) curve to investigate the leakage current and operating voltage of our μLEDs. Optical properties, including the peak wavelength, full-width

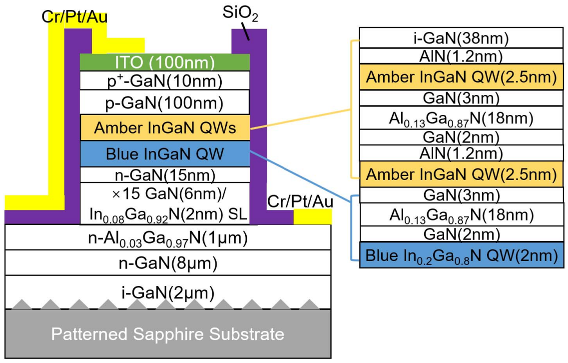

Fig. 1. Schematic structure of InGaN μLED devices.

at half maximum (FWHM), light output power, and on-wafer EQE of the amber μLEDs, were characterized by on-wafer testing. We finally measured temperature-dependent electroluminescence (EL) to evaluate the temperature stability of the μLEDs.

II. Experimental Details

Our amber InGaN LED epitaxial wafers were grown on c-plane patterned sapphire substrates via metalorganic vapor-phase epitaxy. The epitaxial structures have been reported in our previous study [16]. The thick GaN template [16] and hybrid InGaN QWs [20] were used to reduce the lattice mismatch of the InGaN amber QWs. The n-$Al_{0.03}Ga_{0.97}N$ layer could realize an extremely low resistivity by high Si doping [21]. The schematic structure of InGaN μLEDs is shown in Figure 1(a). Indium tin oxide (ITO) was deposited as the transparent conductive layer, and a two-step annealing with and without O_2 gas was done to achieve ohmic contacts with p-GaN [22]. The sheet resistivity of ITO layers could be further improved after the second annealing without O_2 gas. The μLED mesa was formed by etching through the ITO layer, InGaN QWs, and InGaN/GaN superlattices (SLs) to the n-type $Al_{0.03}Ga_{0.97}N$ layer using inductively-coupled plasma. Before fabricating the n- and p-electrodes (Cr/Pt/Au), a SiO_2 layer was deposited using plasma-enhanced chemical vapor deposition to passivate the μLED sidewalls. This SiO_2 layer could also serve as an isolated layer between the p-electrode and n-AlGaN.

The morphology of μLEDs was examined via a scanning electron microscope (SEM). The μLEDs were characterized at a probe station using a semiconductor parameter analyzer. The EL properties were measured under different currents at stage temperatures ranging from 295 K (room temperature) to 373 K.

III. Results and Discussion

Figure 2(a) shows the top-view SEM image of a 47×47 μm^2 μLED. The n-electrode was around the four sidewalls of the μLED, and the p-electrode on ITO was designed as a cross shape. The designs of both the n- and p-electrodes were expected to guarantee uniform current injection into the μLED. Because the p-electrode extended from the bottom to the top of the μLED, the SiO_2 isolated layer covering the sidewall of the μLED was critical to avoid the connection between the p-electrode and the n-AlGaN layer.

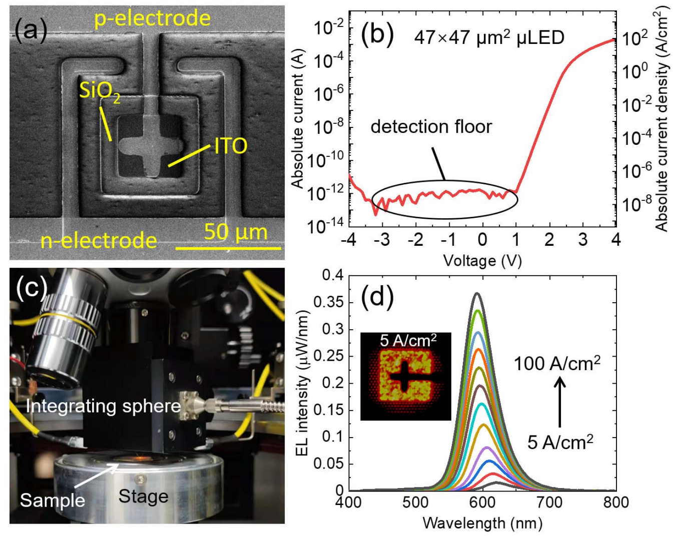

Fig. 2. (a) Top-view SEM image of a 47×47 μm^2 InGaN μLED. (b) Absolute current and current densities of a typical μLED at the different bias voltages. (c) Measurement configuration picture of our μLEDs. (d) EL spectra of a μLED at 5-100 A/cm^2. The inset is the emission image at 5 A/cm^2.

The $|I|$–V curve was measured under the applied voltage ranging from –4 to 4 V. The absolute current was plotted on a logarithmic scale as shown in Figure 2(b). At a forward voltage below 1 V, the absolute current was at the detection floor. After increasing the forward voltage above 1 V, the current was increased linearly with two different slopes on the semi-logarithmic scale. The first linear part corresponded to the tunneling leakage current [23], while the second linear part was the typical operation region of a p-n junction diode. The transition point between the two linear parts, which was regarded as the turn-on voltage, was around 2.5 V. This $|I|$–V behavior was quite similar to other yellow/red InGaN μLEDs [6], [14]. The operating voltage at 20 A/cm^2 was around 3.1 V.

At the reverse voltage, the reverse current also stayed at the detection floor. However, it started to increase after the reverse voltage increased above –3 V. The increment of the reversed currents illustrates that some leakage channels existed in our InGaN μLEDs, which might be caused by the defects in the InGaN active region [24] and the Shockley-Read-Hall (SRH) non-radiative recombination at the μLED sidewalls [9].

Figure 2(c) shows the EL measurement configuration of μLEDs. μLEDs were driven at the probe station, and the integrating sphere was located above the sample to collect the light output power of μLEDs. Figure 2(d) shows the EL spectra of a μLED at 5 to 100 A/cm^2. The typical single peaks can be observed for all EL spectra. The peak wavelength of the μLED was 606 nm at 20 A/cm^2 (non-uniformity $\sim$ 603–611 nm for 2- inch wafer). No additional blue peaks in this work demonstrated less In fluctuation and phase separation in the μLED compared to previous works [16], [25]. The EL emission of the μLED at 5 A/cm^2 in the inset of Fig. 2(d) exhibited non-uniform luminescence due to defects in the amber QWs.

The current density dependence of the peak wavelength and FWHM for the μLEDs is shown in Figure 3(a). The peak wavelength of the μLED exhibited a total 33-nm blue-shift

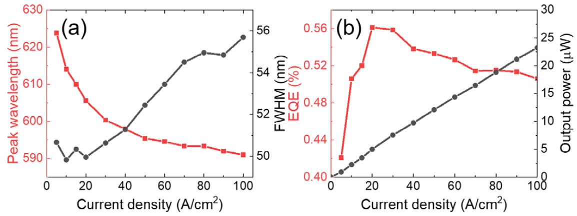

Fig. 3. (a) Peak wavelength and FWHM and (b) EQE and output power of a typical μLED at different current densities based on on-wafer testing.

from 624 to 591 nm at 5 to 100 A/cm^2. However, the blue-shift behavior was different at low and high current densities. At the current densities <40 A/cm^2, the blue-shift of the peak wavelength was as large as 26 nm, which was caused by the strong QCSE and band filling effect in high-In-content InGaN QWs [8], [11], [26]. However, at the current densities above 40 to 100 A/cm^2, the band filling effect should have been negligible, and the QCSE was also partially compensated. Therefore, the peak wavelength of the μLED had a slight blue-shift of 7 nm, as shown in Figure 3(a). Because the QCSE and the band filling effect were respectively originated from the in-plane strain and In fluctuation in InGaN QWs, the strain relaxation and the improvement of the InGaN crystal quality were vital for suppressing this large blue-shift.

The FWHM at the current density below 20 A/cm^2 remained 50-51 nm, which was comparable to the best values of other InGaN orange and red LEDs [15], [27]. However, the FWHM increased to around 56 nm with a current density up to 100 A/cm^2. Our previous work found that the reason was the heat generation in devices under high direct current injection [25].

The output power of the μLED increased almost linearly with the current density. At 20 A/cm^2, we obtained an output power of 5 μW at the wavelength of 606 nm. The output power density was calculated as 2.26 mW/mm^2, which corresponded to the peak on-wafer EQE of 0.56% (Fig. 3(b)).

To estimate the absolute EQE in the integrating sphere, a green μLED in the same size was used to obtain the calibration factor for the on-wafer testing and measurement in the integrating sphere. This calibration method was also used in other works [6], [14]. The output power of the green μLED (bare chip without resin) measured in the integrating sphere was enhanced by ~2.17 compared to that measured by the on-wafer testing. Therefore, we could expect that the absolute peak EQE of our amber μLEDs was estimated to exceed 1.2%. At the current density above 20 A/cm^2, the on-wafer EQE in Fig. 3(b) exhibited a typical behavior of the efficiency droop, which was calculated around 10% from 20 to 100 A/cm^2.

The characteristic temperature indicates the temperature stability of μLEDs [27]. A larger characteristic temperature implies a weaker temperature dependence. The EL intensity of the μLEDs at 20 to 100 A/cm^2 at different stage temperatures from 295 (RT) to 373 K was normalized by EL intensity at RT and plotted on a logarithmic scale in Figure 4(a). The characteristic temperature could be obtained using the following formula shown below:

$$I = I_{T=295K} \exp\left(-\frac{T - 295K}{T_0}\right) \quad (1)$$

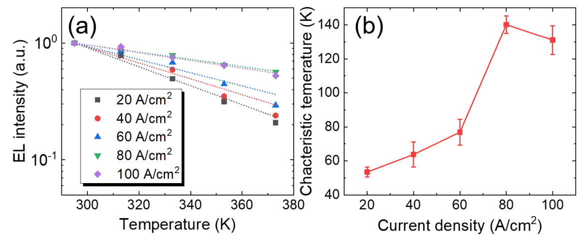

Fig. 4. (a) EL integral intensity of a typical μLED at different current densities. (b) Fitted characteristic temperatures at different current densities.

where I is the normalized EL intensity, $I_{T=295K}$ is the EL intensity at 295 K, T [K] is the stage temperature, and T_0 [K] is the characteristic temperature.

By fitting the experimental data in Figure 4(a), we obtained the characteristic temperatures and their fitting errors at 20 to 100 A/cm^2 in Figure 4(b). The characteristic temperature was 50–80 K at the current density < 60 A/cm^2, but increased strongly to 120–140 K at 80 to 100 A/cm^2. We found that the characteristic temperature of InGaN μLEDs was much lower than our standard red LEDs (higher than 300 K) [25], which was caused by more SRH non-radiative recombination at the sidewalls of μLEDs compared to standard LEDs.

Furthermore, the SRH non-radiative recombination was also the main reason for the current density dependence of the characteristic temperature for InGaN μLEDs [28]. At this point, we believe that the SRH non-radiative recombination included not only the surface recombination at the sidewalls but also the defect-related non-radiative recombination in high-In-content QWs. The SRH non-radiative recombination could be saturated at high current densities. Therefore, the EL intensity of the μLEDs at high current densities would be less influenced by the SRH non-radiative recombination and exhibited less thermal droop and higher characteristic temperatures.

IV. Conclusion

In summary, we demonstrated amber InGaN 47 × 47 μm^2 μLEDs with a wavelength of 606 nm and an FWHM of 50 nm at 20 A/cm^2. A large blue-shift of 33 nm for the amber InGaN μLEDs was observed at 5 to 100 A/cm^2. The peak on-wafer EQE was 0.56% (estimated to exceed 1.2% if measured in the integrating sphere) at 20 A/cm^2, corresponding to a high output power density of 2.26 mW/mm^2. The characteristic temperature was 50–80 K at 20 to 60 A/cm^2 but increased to 120–140 K at 80 to 100 A/cm^2. These higher characteristic temperatures under higher current densities were caused by the saturation of the SRH non-radiative recombination at high current densities.

References

[1] Z. Chen, S. Yan, and C. Danesh, "MicroLED technologies and applications: Characteristics, fabrication, progress, and challenges," *J. Phys. D, Appl. Phys.*, vol. 54, no. 12, Mar. 2021, Art. no. 123001, doi: 10.1088/1361-6463/abcfe4.

[2] H. S. Wasisto, J. D. Prades, J. Gülink, and A. Waag, "Beyond solid-state lighting: Miniaturization, hybrid integration, and applications of GaN nano- and micro-LEDs," *Appl. Phys. Rev.*, vol. 6, no. 4, Dec. 2019, Art. no. 041315, doi: 10.1063/1.5096322.

[3] S. S. Konoplev, K. A. Bulashevich, and S. Y. Karpov, "From large-size to micro-LEDs: Scaling trends revealed by modeling," *Phys. Status Solid (A)*, vol. 215, no. 10, May 2018, Art. no. 1700508, doi: 10.1002/pssa.201700508.

[4] S.-C. Huang, H. Li, Z.-H. Zhang, H. Chen, S.-C. Wang, and T.-C. Lu, "Superior characteristics of microscale light emitting diodes through tightly lateral oxide-confined scheme," *Appl. Phys. Lett.*, vol. 110, no. 2, Jan. 2017, Art. no. 021108, doi: 10.1063/1.4973966.

[5] P. Tian, J. J. D. McKendry, Z. Gong, B. Guilhabert, I. M. Watson, E. Gu, Z. Chen, G. Zhang, and M. D. Dawson, "Size-dependent efficiency and efficiency droop of blue InGaN micro-light emitting diodes," *Appl. Phys. Lett.*, vol. 101, no. 23, Dec. 2012, Art. no. 231110, doi: 10.1063/1.4769835.

[6] S. S. Pasayat, R. Ley, C. Gupta, M. S. Wong, C. Lynsky, Y. Wang, M. J. Gordon, S. Nakamura, S. P. Denbaars, S. Keller, and U. K. Mishra, "Color-tunable $<10\ \mu$m square InGaN micro-LEDs on compliant GaN-on-porous-GaN pseudo-substrates," *Appl. Phys. Lett.*, vol. 117, no. 6, Aug. 2020, Art. no. 061105, doi: 10.1063/5.0011203.

[7] D. Hwang, A. Mughal, C. D. Pynn, S. Nakamura, and S. P. DenBaars, "Sustained high external quantum efficiency in ultrasmall blue III–nitride micro-LEDs," *Appl. Phys. Exp.*, vol. 10, no. 3, 2017, Art. no. 032101, doi: 10.7567/APEX.10.032101.

[8] T. Mukai, M. Yamada, and S. Nakamura, "Characteristics of InGaN-based UV/blue/green/amber/red light-emitting diodes," *Jpn. J. Appl. Phys.*, vol. 38, no. Part 1, No. 7A, pp. 3976–3981, Jul. 1999, doi: 10.1143/JJAP.38.3976.

[9] M. S. Wong, C. Lee, D. J. Myers, D. Hwang, J. A. Kearns, T. Li, J. S. Speck, S. Nakamura, and S. P. DenBaars, "Size-independent peak efficiency of III-nitride micro-light-emitting-diodes using chemical treatment and sidewall passivation," *Appl. Phys. Exp.*, vol. 12, no. 9, Sep. 2019, Art. no. 097004, doi: 10.7567/1882-0786/ab3949.

[10] J. Bai, Y. Cai, P. Feng, P. Fletcher, C. Zhu, Y. Tian, and T. Wang, "Ultrasmall, ultracompact and ultrahigh efficient InGaN micro light emitting diodes (μLEDs) with narrow spectral line width," *ACS Nano*, vol. 14, no. 6, pp. 6906–6911, Jun. 2020, doi: 10.1021/acsnano.0c01180.

[11] B. Damilano and B. Gil, "Yellow–red emission from (Ga,In)N heterostructures," *J. Phys. D, Appl. Phys.*, vol. 48, no. 40, Oct. 2015, Art. no. 403001, doi: 10.1088/0022-3727/48/40/403001.

[12] A. Dussaigne, F. Barbier, B. Damilano, S. Chenot, A. Grenier, A. M. Papon, B. Samuel, B. B. Bakir, D. Vaufrey, J. C. Pillet, A. Gasse, O. Ledoux, M. Rozhavskaya, and D. Sotta, "Full InGaN red light emitting diodes," *J. Appl. Phys.*, vol. 128, no. 13, Oct. 2020, Art. no. 135704, doi: 10.1063/5.0016217.

[13] T. Ozaki, M. Funato, and Y. Kawakami, "Red-emitting $In_xGa_{1-x}N/In_yGa_{1-y}N$ quantum wells grown on lattice-matched $In_yGa_{1-y}N/ScAlMgO_4$(0001) templates," *Appl. Phys. Exp.*, vol. 12, p. 4, 2019, doi: 10.7567/1882-0786/aaf4b1.

[14] S. S. Pasayat, C. Gupta, M. S. Wong, R. Ley, M. J. Gordon, S. P. DenBaars, S. Nakamura, S. Keller, and U. K. Mishra, "Demonstration of ultra-small (<10 μm) 632 nm red InGaN micro-LEDs with useful on-wafer external quantum efficiency ($>$0.2%) for mini-displays," *Appl. Phys. Exp.*, vol. 14, no. 1, 2020, Art. no. 011004, doi: 10.35848/1882-0786/abd06f.

[15] S. Zhang, J. Zhang, J. Gao, X. Wang, C. Zheng, M. Zhang, X. Wu, L. Xu, J. Ding, Z. Quan, and F. Jiang, "Efficient emission of InGaN-based light-emitting diodes: Toward orange and red," *Photon. Res.*, vol. 8, no. 11, pp. 1671–1675, 2020, doi: 10.1364/PRJ.402555.

[16] D. Iida, Z. Zhuang, P. Kirilenko, M. Velazquez-Rizo, M. A. Najmi, and K. Ohkawa, "633-nm InGaN-based red LEDs grown on thick underlying GaN layers with reduced in-plane residual stress," *Appl. Phys. Lett.*, vol. 116, no. 16, 2020, Art. no. 162101, doi: 10.1063/1.5142538.

[17] K. Ohkawa, T. Watanabe, M. Sakamoto, A. Hirako, and M. Deura, "740-nm emission from InGaN-based LEDs on c-plane sapphire substrates by MOVPE," *J. Cryst. Growth*, vol. 343, no. 1, pp. 13–16, Mar. 2012, doi: 10.1016/j.jcrysgro.2011.12.075.

[18] D. Iida, S. Lu, S. Hirahara, K. Niwa, S. Kamiyama, and K. Ohkawa, "Enhanced light output power of InGaN-based amber LEDs by strain-compensating AlN/AlGaN barriers," *J. Cryst. Growth*, vol. 448, pp. 105–108, Aug. 2016, doi: 10.1016/j.jcrysgro.2016.05.023.

[19] S. H. Lee, J. Kim, J. H. Shin, H. E. Lee, I.-S. Kang, K. Gwak, D.-S. Kim, D. Kim, and K. J. Lee, "Optogenetic control of body movements via flexible vertical light-emitting diodes on brain surface," *Nano Energy*, vol. 44, pp. 447–455, Feb. 2018, doi: 10.1016/j.nanoen.2017.12.011.

[20] D. Iida, K. Niwa, S. Kamiyama, and K. Ohkawa, "Demonstration of InGaN-based orange LEDs with hybrid multiple-quantum-wells structure," *Appl. Phys. Exp.*, vol. 9, no. 11, Nov. 2016, Art. no. 111003, doi: 10.7567/APEX.9.111003.

[21] T. Sugiyama, D. Iida, T. Yasuda, M. Iwaya, T. Takeuchi, S. Kamiyama, and I. Akasaki, "Extremely low-resistivity and high-carrier-concentration Si-doped $Al_{0.05}Ga_{0.95}N$," *Appl. Phys. Exp.*, vol. 6, no. 12, Dec. 2013, Art. no. 121002, doi: 10.7567/APEX.6.121002.

[22] Z. Zhuang, D. Iida, P. Kirilenko, M. Velazquez-Rizo, and K. Ohkawa, "Optimal ITO transparent conductive layers for InGaN-based amber/red light-emitting diodes," *Opt. Exp.*, vol. 28, no. 8, pp. 12311–12321, 2020, doi: 10.1364/OE.389725.

[23] T. Zhi, T. Tao, B. Liu, Y. Li, Z. Zhuang, G. Zhang, Z. Xie, R. Zhang, and Y. Zheng, "Asymmetric tunneling model of forward leakage current in GaN/InGaN light emitting diodes," *AIP Adv.*, vol. 5, no. 8, Aug. 2015, Art. no. 087151, doi: 10.1063/1.4929400.

[24] T. Zhi, T. Tao, B. Liu, Z. Xie, P. Chen, and R. Zhang, "Reverse leakage current characteristics of GaN/InGaN multiple quantum-wells blue and green light-emitting diodes," *IEEE Photon. J.*, vol. 8, no. 5, pp. 1–7, Oct. 2016, doi: 10.1109/JPHOT.2016.2600022.

[25] Z. Zhuang, D. Iida, and K. Ohkawa, "Effects of size on the electrical and optical properties of InGaN-based red light-emitting diodes," *Appl. Phys. Lett.*, vol. 116, no. 17, Apr. 2020, Art. no. 173501, doi: 10.1063/5.0006910.

[26] M. Funato, M. Ueda, Y. Kawakami, Y. Narukawa, T. Kosugi, M. Takahashi, and T. Mukai, "Blue, green, and amber InGaN/GaN light-emitting diodes on semipolar 11–22 GaN bulk substrates," *Jpn. J. Appl. Phys.*, vol. 45, no. No. 26, pp. L659–L662, Jul. 2006, doi: 10.1143/JJAP.45.L659.

[27] J.-I. Hwang, R. Hashimoto, S. Saito, and S. Nunoue, "Development of InGaN-based red LED grown on (0001) polar surface," *Appl. Phys. Exp.*, vol. 7, no. 7, Jul. 2014, Art. no. 071003, doi: 10.7567/APEX.7.071003.

[28] D. S. Meyaard, Q. Shan, J. Cho, E. F. Schubert, S.-H. Han, M.-H. Kim, C. Sone, S. J. Oh, and J. Kyu Kim, "Temperature dependent efficiency droop in GaInN light-emitting diodes with different current densities," *Appl. Phys. Lett.*, vol. 100, no. 8, Feb. 2012, Art. no. 081106, doi: 10.1063/1.3688041.